Hagelskjær *et al.*
Microplastics and Nanoplastics (2023) 3:22
https://doi.org/10.1186/s43591-023-00071-5

Microplastics and Nanoplastics

RESEARCH

Open Access

Investigating the correlation between morphological features of microplastics (5–500 µm) and their analytical recovery

O. Hagelskjær[1,2*], A. Crézé[3], G. Le Roux[1] and J. E. Sonke[2]

Abstract

As a direct result of laboratory sample manipulation required to identify microplastics (MPs) within a given matrix, some MPs are inevitably lost. The extent of this loss can be quite significant and varies greatly depending on the sample matrix, choice of protocol and target MPs in question. Defining analytical MP recovery is therefore a critical component in ensuring the quality of MP protocols. The potential relationship between particle size and recovery rate has been widely discussed but remains uncertain. To determine whether MP loss correlated with particle size, three aliquots of polyethylene fragments in the 5–50 µm size range and three aliquots of polypropylene fragments in the 50–500 µm size range, were consecutively transferred back and forth from filter to liquid. After each individual transfer the analytical recovery within specified size groups, was evaluated by applying high-resolution darkfield microscopy. Average recovery across the entire size range was estimated at 80% with a standard deviation (std. dev.) of 26%. Notably, particle coverage on filters (A%) showed a more significant impact on recovery than particle size. Maintaining A% below 5% on filters for microscopic analysis is advised to prevent excessive loss due to particle agglomeration. To determine whether the use of red polyethylene fragments in the 5–50 µm size range in combination with darkfield microscopy could potentially improve MP recovery evaluation in environmental samples, three aliquots of 0.5 g of dry brown trout muscle tissue were spiked and treated according to a relevant protocol. This size-discriminating approach accurately determined average recovery at 52% with a std. dev. of 4% and demonstrated the potential for correction of the concentration enhancement of smaller MPs resulting from particle breakup during sample pre-treatment, which would otherwise lead to overestimation of smaller size fractions.

Highlights

- Recovery experiment shows no evidence of increasing microplastic loss with decreasing particle size, in the 5–500 µm range.
- Investigating colored PE micro-fragments under darkfield illumination enables size-discriminating recovery estimations of microplastics ≥ 5 µm.
- Particle area coverage should not exceed 5% of filters intended for microscopic analysis of microplastics (< 500 µm).

*Correspondence:
O. Hagelskjær
oskar.hagelskjaer@univ-tlse3.fr
Full list of author information is available at the end of the article

• For increased relevance to environmental conditions, fragments should replace spheres or beads in microplastic recovery experiments.

Keywords Positive quality control, Particle coverage (A%), Recovery rate (RR), Fragments, Experiment, Statistics

Introduction

The sample manipulation necessary for isolating microplastics (MPs) in a diverse range of environmental matrices often requires several transfer steps back and forth from filters to liquids [1–3], resulting in the inevitable loss of some MPs [4]. To asses this loss, a recovery rate (RR) experiment using spike MPs can be performed. This procedure is often applied as a positive quality control in environmental MP studies [5]. Establishing RR is critical to accurate MP analysis and research [6–9]. Results from studies not addressing MP recovery may be questionable [10], as the loss of MPs through sample manipulation can be quite significant [5, 11]. RR is often established by adding a known or approximate number of MPs to the matrix in question, executing the relevant protocol and determining or estimating the loss of spiked MPs [12–15]. Designing the ideal MP recovery experiment would require: (i) a large number of MPs to satisfy statistical significance, (ii) a wide size range of MPs, (iii) MPs of varying morphological nature and with varying densities and levels of hydrophobicity as well as MPs containing various dyes and additives, and at different stages of degradation. (iv) The interaction between specific polymers, chemical reagents and laboratory equipment/material used in the relevant protocol is also a critical parameter to consider. However, realizing an experimental setup that addresses all these requirements is challenging and recovery experiments are therefore often simplified in order to achieve feasibility. A typical recovery experiment relies on the addition of a solution containing an approximated number (MPs/mL) of commercial MP spheres in a limited size range [5, 11, 16, 17] and the subsequent approximation of the final number of MPs following the entire protocol; either by visual identification [12, 18], subsampling by vibrational spectroscopy techniques [11] or even weighing [19]. Since natural samples include MPs with highly diverse morphological features, the established RR may not be applicable to all particles. In environmental samples, MP fragments are among the most abundant shapes [20]. Recovery experiments would therefore better mimic true recovery of environmental MPs if the reference MPs were fragments instead of spheres or beads. Another highly critical parameter is particle size. As smaller particles are generally considered to be more mobile, it has been hypothesized that RR decreases with decreasing particle size, and some studies do speculate on, or indicate such a correlation [5, 11, 17, 21–25].

This study aimed to investigate whether particle size and recovery are directly correlated and to further understand what processes and parameters affect MP (< 500 µm) recovery. By implementing image analysis of photomicrographs captured under darkfield illumination, this study investigated whether morphological features such as size, circularity and aspect ratio, directly affected the recovery of MP fragments. Additionally, by spiking three brown trout muscle tissue samples and executing a relevant protocol for MP extraction [1], the study evaluated the applicability of the same MP fragments for more precise and environmentally relevant MP recovery experiments.

Materials and methods

Laboratory procedures

Recovery experiment

Polyvinylidene fluoride (PVDF) filter membranes spiked with a diverse size range of colored polyethylene (PE) and polypropylene (PP) MP fragments were four times transferred back and forth between liquid to filter using glass bottles and a glass vacuum filtration device (Fig. 1) commonly applied in MP isolation procedures [4, 12, 26–33].

After each transfer, morphological features and the number of MPs in the 5–50 and 50–500 µm ranges, in

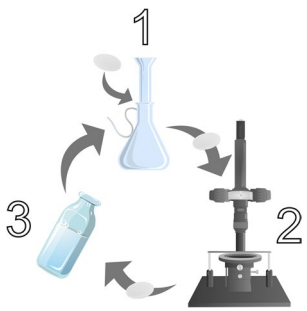

Fig. 1 (1) Using a glass vacuum filtration device, particles were filtered onto a 25 mm, 0.65 µm PVDF filter membrane. (2) Photomicrographs were captured under darkfield illumination in order to determine the quantity and morphological parameters of the transferred MPs. (3) All particles on the examined filter were subsequently flushed with ultrapure Milli-Q water, into a 40 mL glass bottle. The content of the bottle was then poured, flushed and filtered onto another PVDF filter membrane. This process was repeated four times for each sample

size groups at a resolution of 5 and 50 µm, respectively (each group representing 10% of their respective size range), were determined using a ColSpec® MK2 darkfield color-spectral imaging microscope (LightForm, Inc., ColSpec® MK2, Asheville NC USA). The number of particles within the specified size groups before and after each individual transfer were determined to calculate the resulting loss and RR.

MPs are generally defined as plastic particles between 1 µm and 5000 µm (5 mm) in diameter [34] but within the frame of this study, plastics within the 5–50 µm size range will be referred to as fine MP (FMP), while plastics between 50–500 µm will be referred to as small MP (SMP).

To acquire FMPs, Red PE ($\rho = 0.96$ g/cm^3) fragments were produced by manual crushing of 10–27 µm microspheres (CoSpheric LLC, Santa Barbara California USA) using a glass mortar and pestle. The fragments were transferred into a glass bottle containing a 1000 mL solution of prefiltered (pore size = 0.45 µm) ultrapure Milli-Q water (18.2 MΩ·cm) with 5 mL of added surfactant (Sigma-Aldrich, Tween®20, Darmstadt Germany). To further separate individual particles, the bottle and solution was sonicated in two cycles of 30 min. To acquire SMPs, blue PP ($\rho = 0.91$ g/cm^3) fragments were produced by filing a piece of blue virgin macroplastic. These fragments were transferred into another glass bottle and treated in the aforementioned manner.

Three aliquots of 1 mL of FMP solution containing approximately 1500 FMPs/mL were filtered onto individual pre-rinsed 25 mm, 0.65 µm PVDF filter membranes using a glass vacuum filtration device. Similarly, three aliquots of 3 mL SMP solution containing approximately 300 SMPs/mL were transferred onto individual PVDF filter membranes. High-resolution photomicrographic mosaics visualizing the entire surface area of each individual filter, were subsequently obtained, after which the filters were directly transferred into 40 mL glass bottles. Using perfluoroalkoxy alkane (PFA) squeeze bottles containing ultrapure Milli-Q water, the content of the bottle and the filter was once again flushed into a glass vacuum filtration device and onto another pre-rinsed 25 mm, 0.65 µm PVDF filter membrane. The inner walls of the glass bottle as well as of the glass filtration device were flushed with ultrapure Milli-Q water three times to increase the transfer of particles onto the filter surface. The entire process was repeated four times for each aliquot. On the basis of the resulting twelve transfers, average RR within the specified size ranges was determined based on the loss of particles between each individual transfer, illustrated in Fig. 2. By combining the pool of FMP and SMP particles, average recovery of particles based on morphological features independent of size was based on a total of 24 transfers (with exceptions due to insignificant number of particles with specific morphological features). All glassware utilized in the experiment was subjected to kiln sterilization (1h, 500 °C).

MP Recovery in trout muscle tissue

To demonstrate the use of MP fragments in the 5–50 µm size range to determine more environmentally relevant RR within specified size groups, three aliquots of 5 mL of the same FMP solution (~ 1500 FMPs/mL) used in the general recovery experiment (Sect. 2.1.1.), were transferred onto individual pre-rinsed 25 mm, 0.65 µm PVDF filter membranes. Darkfield microscopy was utilized to record the morphological characteristics and quantity of the spike microplastics.

The content of the filters was flushed into 40 mL glass bottles and subsequently poured into three individual 200 mL glass jars, each containing 0.5 g of dried brown trout (*Salmo trutta*) muscle tissue. Only the recovery of FMPs was evaluated, as environmental MPs found within this matrix are almost exclusively below 50 µm in diameter. The samples were treated in accordance of a self-made protocol with inspiration from Dellisanti et al. (2023) [1]. The process involved three steps performed in the following order: (i) Primary matrix removal through the use of 30 vol.% potassium hydroxide (KOH) on a hotplate at 50°C for 24 h, (ii) density separation using zinc chloride ($ZnCl_2$) ($\rho = 1.6$ g/ml) and (iii) digestion of residual organic matter by the use of 30 vol.% hydrogen peroxide (H_2O_2) on a hotplate at 50°C for 7 days.

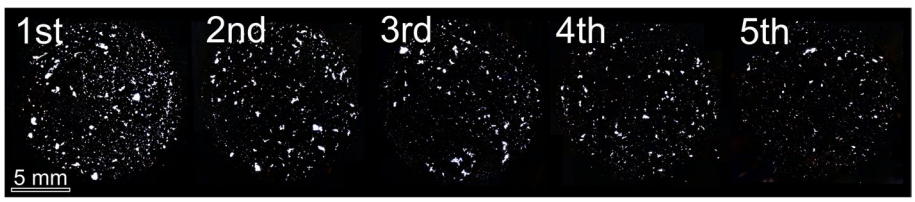

Fig. 2 Mosaics visualizing, from left to right, the evolution of MP loss in sample "SMP1" following each individual transfer. 1st, 2nd etc. refers to 1st filter, 2nd filter and so on

After executing the entire protocol, the contents were filtered onto individual pre-rinsed 25 mm, 0.65 µm PVDF filter membranes and the number and size distribution of remaining FMP particles was then determined using darkfield microscopy to accurately establish the average recovery resulting from the protocol. All glassware utilized in this experiment was also subjected to kiln sterilization (1h, 500 °C).

Image processing and instrumental configuration

Recovery experiment

To register the number of spike MPs and their morphological information, a ColSpec® MK2 darkfield color-spectral imaging microscope was used to obtain the photomicrographs. The distance from the stage to the light-source was adjusted until the filter background displayed almost no reflectance but still allowed the reference MPs of interest to remain clearly visible. Instrumental configurations and parameters were equal between all samples. Using the grid/collection stitching method [35], multiple photomicrographs at a resolution of 1920 × 1200 pixels, were automatically stitched together to form high-resolution mosaics covering the entire filter area. Figure 3 demonstrates how morphological information was extracted from the mosaics. At a resolution of 2.6 µm per pixel, the morphological information of individual particles, was automatically extracted by defining relevant color thresholds in the FIJI ImageJ 1.53t imaging software, that would visually isolate the spike MPs of interest from the background and other generic particles. Particles with Feret diameter below and above 5–50 and 50–500 µm were not considered for FMP and SMP samples, respectively.

MP recovery in trout muscle tissue

Registration of morphological parameters and number of FMP spikes followed the same procedure as the general recovery experiment, with the exception of an increased microscopic resolution of 2.05 µm per pixel, enabling better identification of smaller particles as well as discrimination between individual particles in close proximity. At this resolution, a mosaic covering the same area as in the general recovery experiment (Ø = 1.4 cm), required 40 instead of 24 photomicrographs of similar resolution *i.e.* 1920 × 1200 pixels. Figure 4 illustrates how well the red FMP spikes were visually separated from other generic particles.

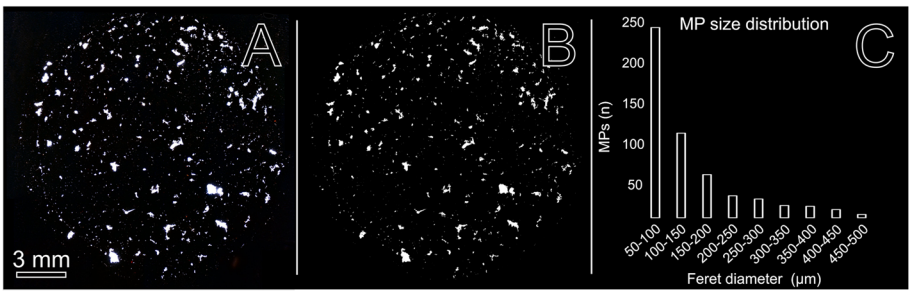

Fig. 3 **A** displays a complete mosaic constructed from 24 photomicrographs, containing highly reflecting blue PP fragments, captured using a ColSpec® MK2 darkfield microscope. Each photomicrograph holds 1920 × 1200 pixels where 1 pixel represents 2.6 µm. **B** subsequently, the mask of defined particles was produced using the Fiji ImageJ 1.53t imaging software from which (**C**) a histogram displaying size distribution of the spike MPs was constructed

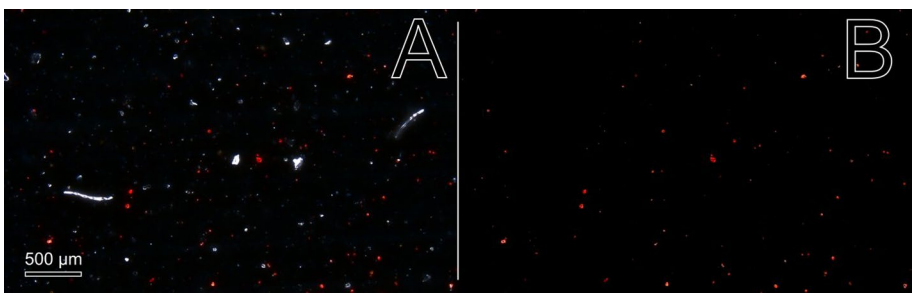

Fig. 4 **A** displays an unaltered photomicrograph of a single frame of a post-protocol FMP sample compared with (**B**), the same frame showing the visually isolated spike MPs, following data treatment

Statistical analysis

Statistical analyses were performed using the R statistical computing software [36] version 4.2.2. Correlations between MP Feret diameter, aspect ratio (AR), circularity, the percentage of filter covered by spike particles (A%) and recovery rate (RR) were calculated for each size group of MPs and individual transfers, using the "Rcorr" function from the "Hmisc" package [37]. The Pearson correlation method was used [38] to calculate both correlations between variables and the *p*-values of the correlations for an alpha value of 0.05. Finally, the "Corrplot" function from the eponymous package [39] was employed to visualize the significant correlations between variables.

Results

Recovery experiment

Figure 5 displays average RR of the analyzed size groups of both FMPs and SMPs, along with standard deviation (std. dev.) and total number of transferred particles within the relevant size groups. Across the entire size range, RR was determined at 80% with an average std. dev. of 26%. Based on statistical analysis, a weak correlation between RR and particle diameter of 0.11 (p-value = 0.11, $n = 216$) was determined, indicating that there was insufficient evidence to suggest any link between the two parameters. For FMPs and SMPs individually, correlations of -0.02 (p-value = 0.56, $n = 108$) and 0.06 (p-value 0.86, $n = 108$) were determined.

Morphological features independent of size *i.e.* circularity and AR, were also correlated with the observed RR (Fig. 6). Average recovery was determined at 80 and 79% with std. dev. values of 33 and 26% for AR and circularity, respectively. Total transfer of particles with AR > 3 was very limited ($n < 500$) and std. dev. therefore increased significantly above this threshold. A greater variability in circularity-values produced less variability overall in the std. dev. The statistical analysis determined insignificant correlations between AR, circularity and RR of 0.06 (p-value = 0.41, $n = 168$) and 0.02 (p-value = 0.82, $n = 144$) for AR and circularity, respectively, indicating that there was insufficient evidence to suggest any correlations.

By performing consecutive transfers of the same samples, the total number of particles and thus the percentage of filter area covered by spike particles (A%), decreased following each transfer. A% prior to transfer was correlated with the resulting RR for FMPs and SMPs, respectively (Fig. 7). For SMPs covering up to 7% of the filter, A% and RR showed an apparent trend ($A\% = -0.09 \cdot RR + 11.58 \leftrightarrow RR = -8.7 \cdot A\% + 115$, $R^2 = 0.80$ ($n = 11$)) and statistical analysis demonstrated significant negative correlation of -0.89 (p-value = $2 \cdot 10^{-4}$, $n = 11$). Similar statistical analysis was applied to FMPs, covering only up to < 0.25% of the filter, but was inconclusive (p-value = 0.9, $n = 12$). A noticeable difference between the spread of points within the primary RR- 'populations' of FMP and SMP samples was also observed. The primary RR population of SMPs was 1.6 times wider than for FMPs and showed no correlation with A%. For FMPs, the three datapoints outside the primary RR-population have been interpreted as random outliers as they do not follow any clear correlation. Amongst SMPs, one outlier was identified. All data

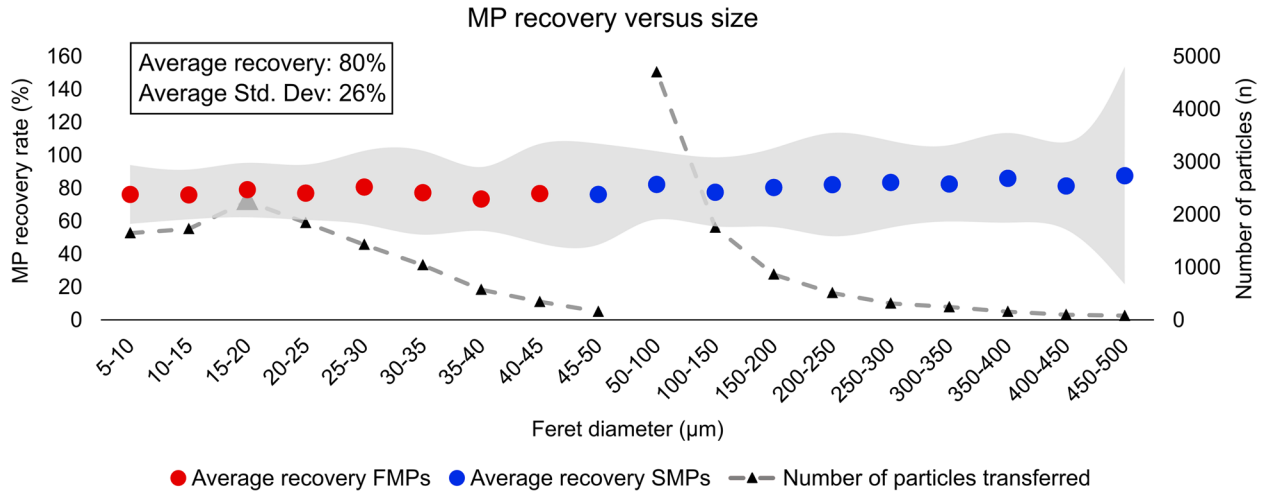

Fig. 5 The diagram plots average recovery rate (RR) of FMPs (5–50 µm) and SMPs (50–500 µm) within specified size groups, based on 12 transfers. The total number of transferred particles within these groups is marked by triangles. Average RR across the entire size range was estimated at 80% with a std. dev. of 26%. No correlation between RR and size could be established

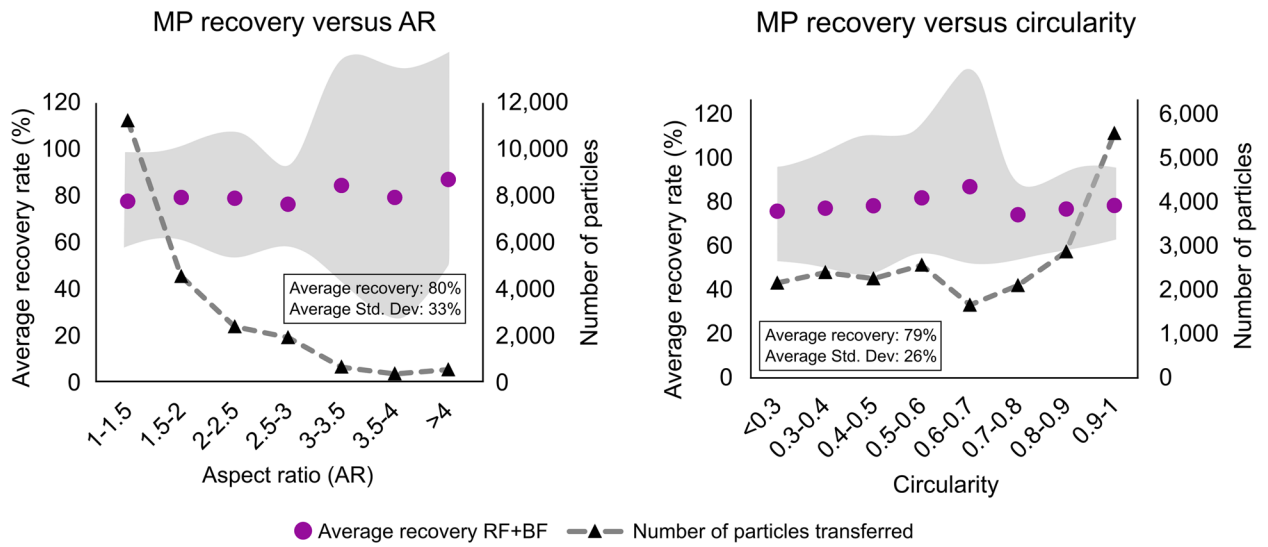

Fig. 6 The diagrams plot average recovery of FMPs and SMPs combined, versus AR (left), and circularity (right). The total number of transferred particles within the specified ranges is marked by black triangles. Average recovery based on AR shows stability around the overall average recovery of 80% at AR < 3. Above this threshold the number of transferred particles becomes statistically insignificant and std. dev. increases significantly. RR of MPs of both high and low circularity showed reasonable stability around the overall average RR of 79%, yet at AR 0.6–0.7, standard deviation increased significantly. Note that high std. dev. coincides with low number of transferred particles

relevant to this experiment is available in the Supporting information 1 (SI1).

MP recovery in trout muscle tissue

Pre-protocol FMP samples 1, 2 and 3 contained $n = 7186$, 7379 and 8219 red PE fragments in the size range of 5–50 µm, respectively, while post-protocol FMP samples contained, in the same size range, $n = 3391$, 4117 and 4465 red PE fragments, respectively. Recovery in FMP samples 1, 2 and 3 was estimated at 47.2, 55.8 and 54.3%, respectively. Average recovery of all spike MPs was thus estimated at 52.4 ± 3.8% (Fig. 8). No significant correlation between MP size and recovery could be established. MP size distribution remained relatively stable across the entire size range. Recovery of the smallest size group (5–10 µm) showed the largest deviation from the mean at 62.8 ± 6.2%. All data relevant to this experiment is available in the supporting information 2 (SI2).

Discussion

Interpretation of results

Recovery experiment

While our findings indicated that there was no correlation between the recovery of MPs (5–500 µm) and size, aspect ratio (< 3) and level of circularity, this disassociation could not be validated by our statistical tests. Despite this, the implications of our results suggest that the likelihood of a MP fragment adhering to glass apertures, filter membranes, or other containers during sample treatment is similar irrespective of morphology.

The available literature presents inconsistent interpretations regarding the correlation between MP size and recovery. While it is generally agreed that MP loss increases as particle size decreases, some studies contradict this notion. For instance, an experiment conducted by Hurley et al. 2018 [16] reported no difference in the recovery of large (850–1000 µm) and small (425–500 µm) PE beads.

Wolff et al., 2021 [40] reported that recovery was not dependent on size by introducing fluorescent PE beads in size ranges of 22–27, 45–53, and 90–106 µm into the samples.

Similarly, Vollertsen and Hansen, 2017 [41] observed no significant difference in the analytical recovery of 100 µm PS spheres and 80–150 µm PE fragments. In fact, another study [24] reported higher RR for the smallest microplastic fraction, which aligns with the results of our experiment on MP recovery in trout muscle tissue.

It is important to note that particle loss can result from factors beyond the mere adhesion of particles. Oversaturation caused by the application of a solution with a concentration of spike MPs can lead to excessive particle agglomeration, resulting in an overestimation of the quantity of larger MPs and, more frequently, an underestimation of smaller particles. To avoid uncertainties in the absolute quantification of initially spiked MPs [17], it is advisable to spike samples with

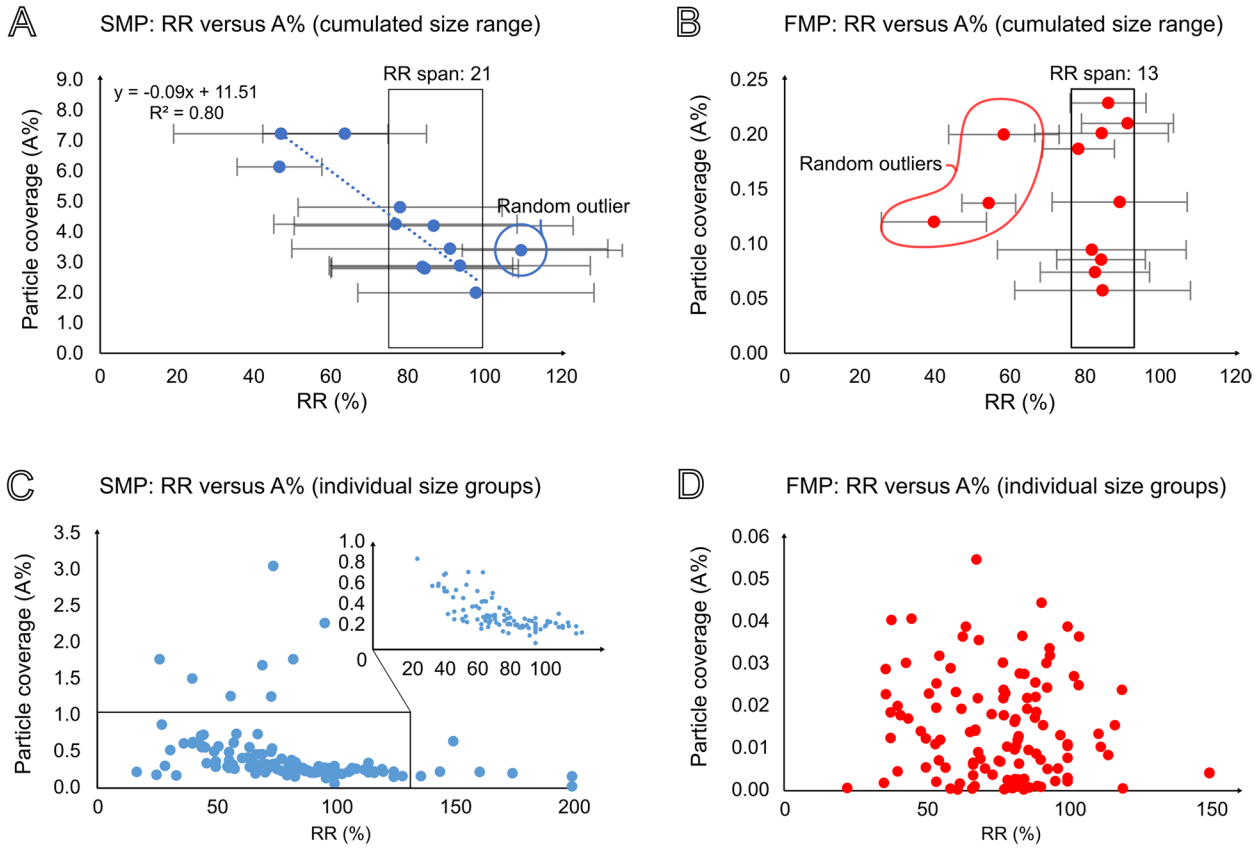

Fig. 7 The diagrams plot particle coverage prior to transfer (A%) against the ensuing RR of each individual transfer. **A** SMPs covering up to 7% of the filter, showed a strong linear correlation ($y = -0.09x + 11.451$, $R^2 = 0.8$) between the two parameters, whereas **B** FMPs covering only up to 0.25% of the filter, showed no correlation. **C** and **D** plot RR versus A% of the individual size groups after each transfer, for FMPs and SMPs, respectively. By removing some outliers in (**C**), the trend becomes more apparent

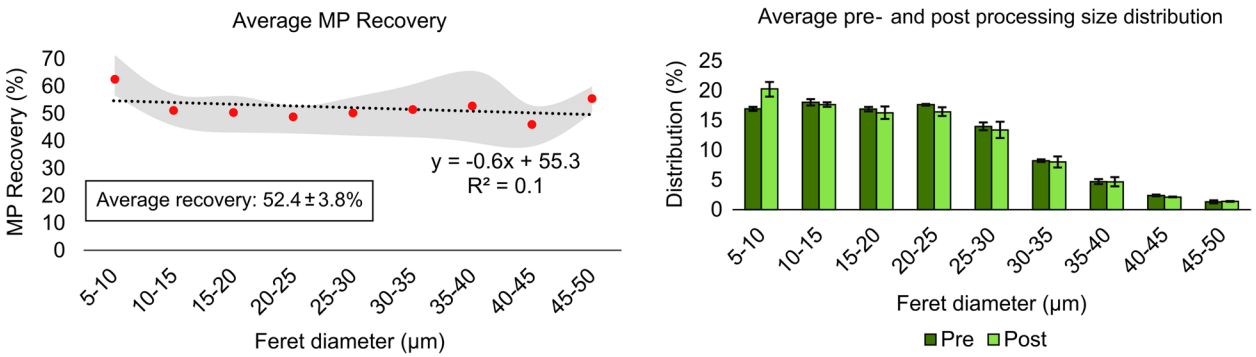

Fig. 8 The diagrams display (left) average RR of FMP fragments at a spatial resolution on the order of 5 µm. Average recovery was estimated at 52.4 ± 3.8% and was largely independent of particle size, with the exception of a noticeable higher RR in the 5–10 µm range. This augmented recovery resulted in a relative concentration enhancement of the smallest size fraction depicted in the histogram (right) displaying average MP size distribution, pre- and post-sample processing. This concentration enhancement may be the result of particle agglomeration and/or particle breakup during sample manipulation

precise quantities of MPs by placing them on a filter and counting them before flushing them into the sample.

Recovery may also be affected by partial or complete disintegration of synthetic polymers in combination with specific chemical reagents [42]. It has

been observed that bases, acids and oxidants become increasingly efficient at decomposing plastics with increasing temperatures [43, 44] and it is reasonable to assume that smaller MPs are more susceptible to partial or complete disintegration due to higher surface area to volume (SA:V) ratios. Temperatures should be limited to 50°C to remain within the heat deflection limits of common MPs [2, 45]. Furthermore, different types of sample matrices and resulting pre-treatment protocols will also affect the recovery of MPs [5, 46]. From personal experience we recognize that increasingly organic rich and complex mediums will negatively affect recovery because (i) they require more intricate laboratory treatment, thus increasing the number of transfer steps and (ii) if complete matrix removal is not achieved, MPs may be concealed, agglomerated or removed with the matrix. MP concealment and agglomeration is particularly relevant for smaller particles [21] and this interpretation was also supported by our experimental data, that showed a strong correlation between RR and A%, where $RR = -8.7 \cdot A\% + 115$ ($R^2 = 0.8$) (Fig. 7). The equation shows that RR decreases as a function of increasing A%. Results of this study demonstrate that it is unadvisable to saturate more than 5% of the area of filter intended for microscopic analysis, in order to avoid an additional loss of particles.

The width of the primary RR population of SMPs was 1.6 times wider than of FMPs (Fig. 7), which may be linked to decreasing RR with increasing A%, and could explain why std. dev. is generally higher above in SMPs. The much smaller FMP fragments occupied considerably less surface area than SMP fragments, and as a result, no correlation between A% and RR could be established for FMPs. To better understand what processes link MP loss and A%, Fig. 9 visualizes the distribution of MPs, following each individual transfer for both FMPs and SMPs.

The histograms illustrate that the distribution of particles across size groups, show very little variation. This again indicates that individual particle size has little to no influence on RR. for SMPs however, when A% decreased, the concentration of the smallest size fraction generally increased in all three experiments. While this apparent trend was not observed in FMPs, we hypothesized a link between high A% and increased probability of particle overlap, concealment and agglomeration (Fig. 10), thereby reducing the analytical recovery of the smallest MP fraction.

Potential breakup of MPs could be a cause of concentration enhancement of the smallest size fraction; however, the sampling protocol was very mild and general concentration enhancement was not observed in the for FMPs in the general recovery experiment. Together, these processes may further contribute to increased uncertainty of RR for SMPs (Fig. 5).

MP recovery in trout muscle tissue

By spiking three individual trout muscle tissue samples and performing an extensive protocol for MP isolation, an average RR of 52.4 ± 3.8% was established. Because we spiked with thousands of MP fragments from 5 to 50 µm, we were able to determine the analytical recovery within specified size groups with low uncertainty. Using this approach enables more precise and environmentally relevant estimations of MP recovery. The proof-of-principle samples indicate the benefits of employing a precise number of MP fragments for recovery experiments, instead of relying on solutions with estimated concentrations of spike particles.

We suggest an individualized size-discriminating approach to recovery estimation, where RR is determined within specified size groups. However, if the difference in RR between size groups is insignificant compared to the overall std. dev., then it would be sufficient to apply the average RR to all MPs.

In this experiment, average RR of MPs in the 5–10 µm size range was noticeably higher (62.8 ± 6.4%) than the overall average RR of 52.4 ± 3.8%, resulting in a relative increase in the proportion of the smallest size group (Fig. 8). This increase could be the result of particle overlap, concealment and agglomeration, yet A% was only 1.3 and 0.6% before and after the protocol, respectively. Therefore, according to Fig. 9, A% should not be influential on RR. It is also possible that the increase was derived from the breakup of particles during sample preparation [41]. If so, then it must also be true for the environmental MPs within. The individualized size-discriminating approach thus enables the correction of MP breakup during sample preparation, which would otherwise lead to overestimation of smaller size fractions.

Study limitations

Recovery experiment

We recognize that the large RR uncertainty for both FMPs and SMPs could be linked to the fact that particle loss during sample manipulation is heavily influenced by randomness. Combined with this high degree of coincidence, the uncertainties of our statistical analyses could be due to a lack of data so a higher number of replicates would likely have decreased the margin of error. Therefore, it would be interesting to increase the number of transfers to determine whether statistical validity improves. It would also be beneficial to increase microscopic size resolution in order to enable better identification of smaller particles as well as discrimination between individual particles in close proximity. Furthermore, it

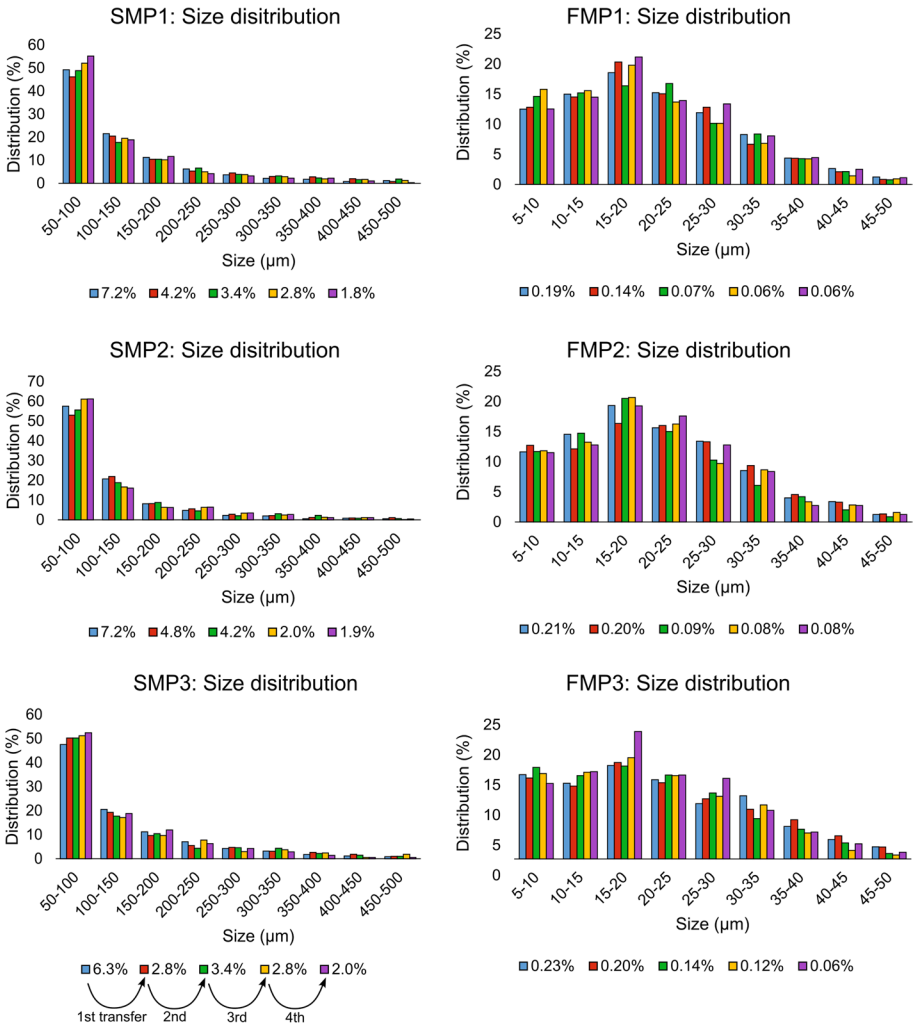

Fig. 9 Histograms visualizing the MP distribution within specified size groups, following each individual transfer. legends refer to the filter area occupied by particles (A%). Size distribution of MPs remains relatively stable following four successive transfers, yet SMPs display an increase in the smallest size fraction with decreasing A%. As a general trend, this tendency was not observed in FMPs and may therefore be linked to excessive A%, leading to increased probability of particle agglomeration and concealment

could be relevant to experiment with individual stages of a typical MP protocol *i.e.* digestion, density separation, etc., in order to determine their respective impact on MP loss. The color of the spike particles may also have an effect on the analytical recovery. Comparing the recovery of the same protocol using different colored particles within the same size range, could be interesting to help determine which color is best suited for recovery experiments of this nature *i.e.* optical microscopy.

The current study only considered the recovery of plastics with densities below 1 g/cm^3*i.e.* PE and PP. These polymers were deliberately chosen due to simplicity and because they comprise 50% of all plastic production [47]. Additionally, PE is the prevailing plastic found in environmental samples within this size range [12, 48]. However, the intrinsic properties of plastics may influence their analytical recovery and the recovery of individual polymers may vary depending on the protocol of choice and the chemical reagents applied. Additionally, during sample treatment, the matrix in question may interact with the polymers within. Therefore, it is possible that a relationship between MP size and RR could exist under specific conditions; distinct from the current experiment conducted in a water medium, and later fish muscle tissue.

MP recovery in trout muscle tissue

To increase homogeneity of RR between the three replicates, the trout muscle tissue samples were spiked with 5 mL of FMP solution and the filters were investigated at a higher microscopic resolution compared to the general recovery experiment. A comparative reduction in std.

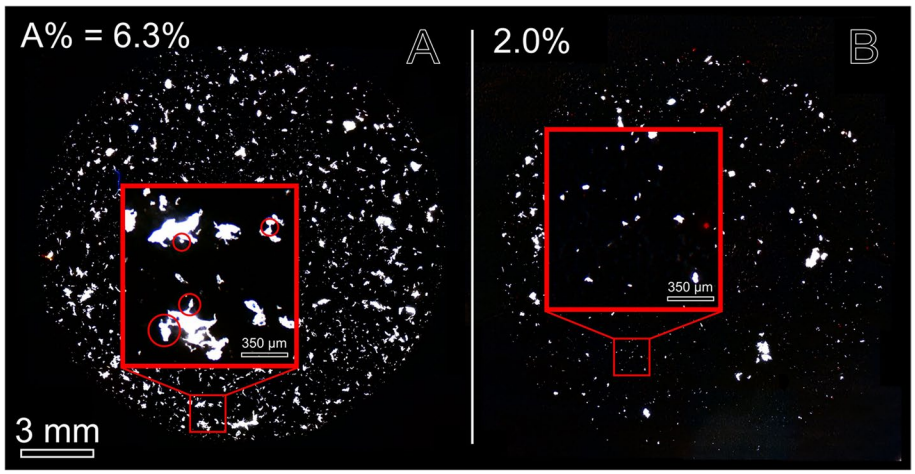

Fig. 10 Photomicrographs visualizing the difference between the potential of particle overlap, concealment and agglomeration when (**A**) A% = 6.3% versus (**B**) A% = 2.0%. Red rings indicate episodes where smaller particles have agglomerated onto larger particles, thereby causing underestimation of the number of smaller MPs. When the filter is less charged, this is probabilistically less likely to occur

dev. was successfully achieved but an elevated number of particles may have contributed to higher probability of particle agglomeration prior to sample treatment. Agglomeration leads to positive bias in the concentration of larger MPs and an even more pronounced negative bias in the concentration of smaller MPs. Up-concentration of small MPs was not observed in the general recovery experiment using the same red PE fragments and may thus be linked to oversaturation of the filter. However, the A% was relatively low (≤ 1.3) and as opposed to the general recovery experiment, FMP spikes were here exposed to strong bases and oxidants. As a result, it is also possible that this concentration enhancement was completely or partly due to particle breakup during sample pre-treatment. For future reference, spiking with half the number of FMP particles, corresponding to A% < 0.7, would likely be sufficient in order to retain statistical significance whilst reducing the potential for particle overlap, concealment and agglomeration as illustrated in Fig. 10.

Recommendations and future considerations

Limiting the particle area coverage on the filter intended for microscopic analysis is already suggested and practiced [49, 50] but no recommendation on a threshold value has yet been proposed. We therefore, suggest based on our findings, that A% on any filter intended for microscopic analysis of SMPs, should not exceed 5% of the total area of the filter. If this threshold is respected, particles should have sufficient spread to reliably represent MPs of all size ranges, whilst decreasing the probability of a significant, additional loss. Figure 11 displays a range of complex environmental samples along with their respective A% following complete sample pre-treatment.

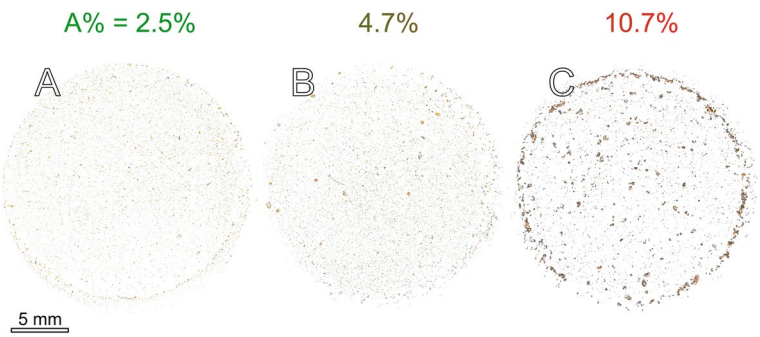

Fig. 11 Photomicrographic mosaics captured under darkfield illumination of pre-treated sphagnum moss samples on 25 mm filter membranes. All particles have been visually isolated from the filter background. This figure serves as a visual guideline for target A%, which should not surpass 5% on filters intended for microscopic analysis of MPs below 500 µm in diameter. A% is acceptable for samples (**A**) and (**B**), whereas (**C**) should not be analyzed

We encourage limiting the amount of sample to treat, to avoid producing 'filter cakes' [51, 52] between transfers. As MP recovery is also largely influenced by coincidence, we recommend that RR should be based on the average recovery of at least three spiked samples. RR must be determined for any specific protocol and spike MPs must be suspended in the relevant sample matrix material. Samples should be spiked with a known number of MPs with known sizes and at a quantity that does not invoke filter supersaturation [53]. If the use of fragments is unfeasible, it would be beneficial to replicate the recovery experiment with two groups of different size ranges of MP spheres or beads [17, 40].

Knowing that MPs interact by Van der Waal's force [54, 55] and static electricity [56], it is reasonable to assume that fragments exhibiting high SA:V ratios are more prone to adhesion than spheres and beads. Considering that the vast majority of MPs (< 500 µm) found in natural samples are fragments or films [20, 57–59], it would be highly relevant to employ the use of fragments instead of beads or spheres for MP recovery experiments [60]. However, depending on the dominant MP morphology in a given sample matrix, spiking with fragments may not always be comprehensive. For instance, it is not unreasonable to assume that fibers and fragments may behave differently from one another during sample treatment. Recovery experiments should be designed to replicate the conditions of the original sample. Therefore, if the sample contains both fibers and fragments which are morphologically dissimilar, it may be beneficial to determine the individual recovery of each morphological type.

A promising technique with the potential to improve the accuracy of dosing and production of reference MPs, is laser microdissection pressure catapulting (LMPC) [61]. Yet, the technique is still relatively slow, dosing at 1 MP/minute. The synthesis of metal-doped plastics [62] is an ingenious way of determining the mass of recovered plastics, even on the nanoscale. The technique however, does not provide morphological information on the individual particles. However, by combining these methods and performing darkfield microscopy on doped MPs, more accurate recovery data may be obtainable. Ongoing research is crucial to enhance our analytical techniques, enabling us to attain more accurate assessments of environmental microplastic pollution [4, 8, 63].

On the basis of our findings and those of other studies [6, 8, 49, 50, 53], we suggest that MP recovery experiments should try to respect the following recommendations: (i) The precise number of initially added spike MPs should be known. (ii) The recovery experiment should be replicated at least three times. (iii) Spike with a significant number of fragments in different sizes, in order to establish RR within specified size groups. If the use of fragments is not feasible, spike with at least two different size groups of spheres or beads. (iv) The size of the spike MPs should match the approximate size of the relevant environmental MPs.

Conclusions

Based on data from twelve transfers between filters, liquids and inversely, the average recovery rate (RR) of polyethylene (PE) and polypropylene (PP) microplastic (MP) fragments in the 5–500 µm size range was estimated at 80 ± 26%. Statistical analysis indicated that there was insufficient evidence to suggest any correlation between RR and particle size (0.11, p-value = 0.11, n = 216). Although this apparent disassociation could not be validated by our statistical tests, the experiment indicated that the recovery of MPs (< 500 µm) was largely independent of size, aspect ratio (< 3) and level of circularity. These results imply that the probability of whether a MP fragment will adhere to glass apertures, filter membranes or other containers during sample treatment, is similar irrespective of morphology.

Sample treatment of a spiked proof-of-principle trout muscle tissue sample did however, exhibit an elevated RR in the smallest size group (5–10 µm) of 63 ± 6%, compared to the average RR of all particles (5–50 µm) of 52 ± 4%. This led to a relative concentration enhancement of the smallest MP fraction which may have resulted from particle overlap, concealment and agglomeration due to spike MP oversaturation of the initial filter but could also stem from particle breakup during sample pre-treatment. Regardless of the cause, this individualized size-discriminating approach has the capacity to enable the correction of potential particle breakup which would otherwise lead to overestimation of the smaller size fractions.

Furthermore, independent of particle size, RR is strongly affected by excessive particle filter coverage (A%). If A% remains below 5%, MPs should have sufficient spread to reliably represent all present size ranges whilst avoiding excessive MP loss. We therefore strongly advice against exceeding A% > 5% on any filter intended for microscopic analysis of MPs (< 500 µm). Finally, we suggest that MP recovery experiments should try to respect the following recommendations: (i) The precise number of initially added spike MPs should be known. (ii) The recovery experiment should be replicated at least three times. (iii) Spike with a significant number of fragments in different sizes, in order to establish RR within specified size groups. If the use of fragments is not feasible, spike with at least two different size groups of spheres or beads. (iv) The size of the spike MPs should match the approximate size of the relevant environmental MPs.

Abbreviations

MP	Microplastic
FMP	Fine microplastic
SMP	Small microplastic
RR	Recovery rate
AR	Aspect ratio
A%	Percentage of filter covered by particles
PE	Polyethylene
PP	Polypropylene
PVDF	Polyvinylidene fluoride
PFA	Perfluoroalkoxy alkane
FTIR	Fourier-transform infrared

Supplementary Information

The online version contains supplementary material available at https://doi.org/10.1186/s43591-023-00071-5.

Additional file 1. SI1 contains all data relevant to the general recovery experiment.

Additional file 2. SI2 contains all data relevant to the proof-of-principle recovery experiment, performed on brown trout muscle tissue.

Acknowledgements
We thank Jeremy M. Lerner for his critical review of the final version of the manuscript and LightForm®, inc. for their ongoing technical support. We also thank Henar Margenat, Nadiia Yakovenko, Lucia Perez Serrano, Faten Mkachar and Théo Segur for scientific discussion. Lastly, we would like to extend our gratitude to three anonymous reviewers, whose thorough revision helped to improve the quality of the manuscript and study.

Authors' contributions
O.H. conceptualized and administered the project, led the laboratorial work, produced and interpreted data and led manuscript writing with help from A.C. who was in charge of the statistical analyses. J.E.S and G.L.R. secured the funding, supervised the project and provided critical revision of the manuscript.

Funding
This work and the PhD fellowship of O.H. is funded by an 80Prime CNRS grant «4DµPlast» (G.L.R, J.E.S.). This publication was supported by ANR-20-CE34-0014 ATMO-PLASTIC (G.L.R, J.E.S.) and the Plasticopyr project within the Interreg V-A Spain-France-Andorra program (G.L.R) as well as observatoire Homme-Milieu Pyrénées Haut Vicdessos—LABEX DRIIHM ANR-11-LABX0010 (G.L.R).

Availability of data and materials
All data generated during this study is included in the published article and its supplementary information files.

Declarations

Ethics approval and consent to participate
Not applicable.

Consent for publication
Not applicable.

Competing interests
The authors declare no competing interests.

Author details
[1]Université de Toulouse, CNRS UMR5245, Laboratoire Écologie Fonctionnelle Et Environnement, Avenue de L'Agrobiopole, 31326 Toulouse, France. [2]CNRS UMR5563 - IRD UR 234, Géosciences Environnement Toulouse, Université Paul Sabatier, 14 Avenue Edouard Belin, 31400 Toulouse, France. [3]Arvalis, Institut du Végétal. 6 Chemin de La Côté Vieille, 31450 Baziège, France.

Received: 23 May 2023 Accepted: 15 September 2023
Published online: 26 September 2023

References

1. Dellisanti W, Leung MM-L, Lam KW-K, Wang Y, Hu M, Lo HS, et al. A short review on the recent method development for extraction and identification of microplastics in mussels and fish, two major groups of seafood. Mar Pollut Bull. 2023;186:114221.
2. Radford F, Zapata-Restrepo LM, Horton AA, Hudson MD, Shaw PJ, Williams ID. Developing a systematic method for extraction of microplastics in soils. Anal Methods. 2021;13:1695–705.
3. Rist S, Vianello A, Winding MHS, Nielsen TG, Almeda R, Torres RR, et al. Quantification of plankton-sized microplastics in a productive coastal Arctic marine ecosystem. Environ Pollut. 2020;266:115248.
4. Dimante-Deimantovica I, Suhareva N, Barone M, Putna-Nimane I, Aigars J. Hide-and-seek: Threshold values and contribution towards better understanding of recovery rate in microplastic research. MethodsX. 2022;9:101603.
5. Way C, Hudson MD, Williams ID, Langley GJ. Evidence of underestimation in microplastic research: A meta-analysis of recovery rate studies. Sci Total Environ. 2022;805:150227.
6. Primpke S, Booth A, Gerdts G, Gomiero A, Kögel T, Lusher A, et al. Monitoring of microplastic pollution in the Arctic: Recent developments in polymer identification, quality assurance and control (QA/QC), and data reporting. Arctic Science. 2022;9(1):176–97. https://doi.org/10.1139/as-2022-0006.
7. Schymanski D, Oßmann B, Benismail N, Kada B, Dallmann G, von der Esch E, et al. Analysis of microplastics in drinking water and other clean water samples with micro-Raman and micro-infrared spectroscopy: minimum requirements and best practice guidelines. Anal Bioanal Chem. 2021;413:5969–94. https://doi.org/10.1007/s00216-021-03498-y.
8. Shruti VC, Kutralam-Muniasamy G. Blanks and bias in microplastic research: Implications for future quality assurance. Trends Environ Anal Chem. 2023;38:e00203.
9. Thiele CJ, Hudson MD, Russell AE. Evaluation of existing methods to extract microplastics from bivalve tissue: Adapted KOH digestion protocol improves filtration at single-digit pore size. Mar Pollut Bull. 2019;142:384–93.
10. Miller ME, Kroon FJ, Motti CA. Recovering microplastics from marine samples: A review of current practices. Mar Pollut Bull. 2017;123:6–18.
11. Weber F, Kerpen J. Underestimating microplastics? Quantification of the recovery rate of microplastic particles including sampling, sample preparation, subsampling, and detection using µ-Ramanspectroscopy. Analytical and Bioanalytical Chemistry. 2022; Available from: https://doi.org/10.1007/s00216-022-04447-z.
12. Hagelskjær O, Le Roux G, Liu R, Dubreuil B, Behra P, Sonke JE. The recovery of aerosol-sized microplastics in highly refractory vegetal matrices for identification by automated Raman microspectroscopy. Chemosphere. 2023;328:138487.
13. Nuelle M-T, Dekiff JH, Remy D, Fries E. A new analytical approach for monitoring microplastics in marine sediments. Environ Pollut. 2014;184:161–9.
14. Pagter E, Frias J, Nash R. Microplastics in Galway Bay: A comparison of sampling and separation methods. Mar Pollut Bull. 2018;135:932–40.
15. Zhu X. Optimization of elutriation device for filtration of microplastic particles from sediment. Mar Pollut Bull. 2015;92:69–72.
16. Hurley RR, Lusher AL, Olsen M, Nizzetto L. Validation of a Method for Extracting Microplastics from Complex, Organic-Rich Environmental Matrices. Environ Sci Technol. 2018;52:7409–17.
17. Weber F, Kerpen J, Wolff S, Langer R, Eschweiler V. Investigation of microplastics contamination in drinking water of a German city. Sci Total Environ. 2021;755:143421.
18. Miller ME, Motti CA, Menendez P, Kroon FJ. Efficacy of Microplastic Separation Techniques on Seawater Samples: Testing Accuracy Using High-Density Polyethylene. Biol Bull. 2021;240:52–66.
19. Fuller S, Gautam A. A Procedure for Measuring Microplastics using Pressurized Fluid Extraction. Environ Sci Technol. 2016;50:5774–80.
20. Boettcher H, Kukulka T, Cohen JH. Methods for controlled preparation and dosing of microplastic fragments in bioassays. Sci Rep. 2023;13:5195.
21. Bottone A, Boily J-F, Shchukarev A, Andersson PL, Klaminder J. Sodium hypochlorite as an oxidizing agent for removal of soil organic matter before microplastics analyses. J Environ Qual. 2022;51:112–22.
22. Estahbanati S, Fahrenfeld NL. Influence of wastewater treatment plant discharges on microplastic concentrations in surface water. Chemosphere. 2016;162:277–84.

23. Liu M, Song Y, Lu S, Qiu R, Hu J, Li X, et al. A method for extracting soil microplastics through circulation of sodium bromide solutions. Sci Total Environ. 2019;691:341–7.
24. Quinn B, Murphy F, Ewins C. Validation of density separation for the rapid recovery of microplastics from sediment. Anal Methods. 2017;9:1491–8.
25. Wang Z, Taylor SE, Sharma P, Flury M. Poor extraction efficiencies of polystyrene nano- and microplastics from biosolids and soil. PLoS One. 2018;13:e0208009.
26. Alfaro-Núñez A, Astorga D, Cáceres-Farías L, Bastidas L, Soto Villegas C, Macay K, et al. Microplastic pollution in seawater and marine organisms across the Tropical Eastern Pacific and Galápagos. Sci Rep. 2021;11:6424.
27. Crawford CB, Quinn B. 9 - Microplastic separation techniques. In: Crawford CB, Quinn B, editors. Microplastic Pollutants. Elsevier; 2017. 203–18. Available from: https://www.sciencedirect.com/science/article/pii/B9780128094068000098.
28. Dong M, Luo Z, Jiang Q, Xing X, Zhang Q, Sun Y. The rapid increases in microplastics in urban lake sediments. Sci Rep. 2020;10:848.
29. Gaston E, Woo M, Steele C, Sukumaran S, Anderson S. Microplastics Differ Between Indoor and Outdoor Air Masses: Insights from Multiple Microscopy Methodologies. Appl Spectrosc. 2020;74:1079–98.
30. Nel HA, Chetwynd AJ, Kelleher L, Lynch I, Mansfield I, Margenat H, et al. Detection limits are central to improve reporting standards when using Nile red for microplastic quantification. Chemosphere. 2021;263:127953.
31. Stanton T, Johnson M, Nathanail P, Gomes RL, Needham T, Burson A. Exploring the Efficacy of Nile Red in Microplastic Quantification: A Costaining Approach. Environ Sci Technol Lett. 2019;6:606–11.
32. Xu Q, Gao Y, Xu L, Shi W, Wang F, LeBlanc GA, et al. Investigation of the microplastics profile in sludge from China's largest Water reclamation plant using a feasible isolation device. J Hazard Mater. 2020;388:122067.
33. Yang J, Monnot M, Sun Y, Asia L, Wong-Wah-Chung P, Doumenq P, et al. Microplastics in different water samples (seawater, freshwater, and wastewater): Methodology approach for characterization using micro-FTIR spectroscopy. Water Res. 2023;232:119711.
34. Hale RC, Seeley ME, Guardia MJL, Mai L, Zeng EY. A Global Perspective on Microplastics. J Geophys Res. 2020;125:e2018JC014719.
35. Preibisch S, Saalfeld S, Tomancak P. Globally optimal stitching of tiled 3D microscopic image acquisitions. Bioinformatics. 2009;25:1463–5.
36. R Core Team. R: A language and environment for statistical computing. R Foundation for Statistical Computing, Vienna, Austria. 2021; Available from: https://www.R-project.org/.
37. Harrel JrF, Dupont Ch. Hmisc: Harrell Miscellaneous_. R package version 4.7–1. 2019; Available from: https://CRAN.R-project.org/package=Hmisc.
38. Benesty J, Chen J, Huang Y, Cohen I. Pearson Correlation Coefficient. Noise Reduction in Speech Processing. Berlin, Heidelberg: Springer Berlin Heidelberg; 2009. p. 1–4. https://doi.org/10.1007/978-3-642-00296-0_5.
39. Wei T, Simko V. R package "corrplot": Visualization of a Correlation Matrix (Version 0.92). 2021; Available from: https://github.com/taiyun/corrplot.
40. Wolff S, Weber F, Kerpen J, Winklhofer M, Engelhart M, Barkmann L. Elimination of Microplastics by Downstream Sand Filters in Wastewater Treatment. Water. 2021;13. Available from: https://www.mdpi.com/2073-4441/13/1/33.
41. Vollertsen J, Hansen AA, editors. Microplastic in Danish wastewater: Sources, occurrences and fate. The Danish Environmental Protection Agency. 2017. p. 55. (Environmental Project, Vol. 1906).
42. Liu B, Jiang Q, Qiu Z, Liu L, Wei R, Zhang X, et al. Process analysis of microplastic degradation using activated PMS and Fenton reagents. Chemosphere. 2022;298:134220.
43. Karami A, Golieskardi A, Choo CK, Romano N, Ho YB, Salamatinia B. A high-performance protocol for extraction of microplastics in fish. Sci Total Environ. 2017;578:485–94.
44. Pfeiffer F, Fischer EK. Various Digestion Protocols Within Microplastic Sample Processing—Evaluating the Resistance of Different Synthetic Polymers and the Efficiency of Biogenic Organic Matter Destruction. Front Environ Sci. 2020;8:263.
45. Qiu Q, Tan Z, Wang J, Peng J, Li M, Zhan Z. Extraction, enumeration and identification methods for monitoring microplastics in the environment. Estuar Coast Shelf Sci. 2016;176:102–9.
46. F.M, Santana M, Kroon FJ, van Herwerden L, Vamvounis G, Motti CA. An assessment workflow to recover microplastics from complex biological matrices. Mar Pollut Bull. 2022;179:113676.
47. PlasticsEurope. Plastic - the facts 2021. 2021.
48. Li C, Gan Y, Zhang C, He H, Fang J, Wang L, et al. "Microplastic communities" in different environments: Differences, links, and role of diversity index in source analysis. Water Res. 2021;188:116574.
49. Bergmann M, Mützel S, Primpke S, Tekman MB, Trachsel J, Gerdts G. White and wonderful? Microplastics prevail in snow from the Alps to the Arctic. Science Advances. 2019;5:eaax1157.
50. Bergmann M, Wirzberger V, Krumpen T, Lorenz C, Primpke S, Tekman MB, et al. High Quantities of Microplastic in Arctic Deep-Sea Sediments from the HAUSGARTEN Observatory. Environ Sci Technol. 2017;51:11000–10.
51. Ba geri BS, Al-Mutairi SH, Mahmoud MA. Different Techniques for Characterizing the Filter Cake. 2013 [cited 2023 Feb 15]. p. SPE-163960-MS. Available from: https://doi.org/10.2118/163960-MS.
52. Ochoa George PA, Eras JJC, Gutierrez AS, Hens L, Vandecasteele C. Residue from Sugarcane Juice Filtration (Filter Cake): Energy Use at the Sugar Factory. Waste Biomass Valorization. 2010;1:407–13.
53. Cabernard L, Roscher L, Lorenz C, Gerdts G, Primpke S. Comparison of Raman and Fourier Transform Infrared Spectroscopy for the Quantification of Microplastics in the Aquatic Environment. Environ Sci Technol. 2018;52:13279–88.
54. Rout S, Yadav S, Joshi V, Karpe R, Pulhani V, Kumar AV. Microplastics as vectors of radioiodine in the marine environment: A study on sorption and interaction mechanism. Environ Pollut. 2022;307:119432.
55. Wang F, Zhang M, Sha W, Wang Y, Hao H, Dou Y, et al. Sorption Behavior and Mechanisms of Organic Contaminants to Nano and Microplastics. Molecules. 2020;25. Available from: https://www.mdpi.com/1420-3049/25/8/1827.
56. Sobhani Z, Lei Y, Tang Y, Wu L, Zhang X, Naidu R, et al. Microplastics generated when opening plastic packaging. Sci Rep. 2020;10:4841.
57. Allen D, Allen S, Le Roux G, Simonneau A, Galop D, Phoenix VR. Temporal Archive of Atmospheric Microplastic Deposition Presented in Ombrotrophic Peat. Environ Sci Technol Lett. 2021;8:954–60.
58. Negrete Velasco A de J, Rard L, Blois W, Lebrun D, Lebrun F, Pothe F, et al. Microplastic and Fibre Contamination in a Remote Mountain Lake in Switzerland. Water. 2020;12. Available from: https://www.mdpi.com/2073-4441/12/9/2410.
59. Stefánsson H, Peternell M, Konrad-Schmolke M, Hannesdóttir H, Ásbjörnsson EJ, Sturkell E. Microplastics in Glaciers: First Results from the Vatnajökull Ice Cap. Sustainability. 2021;13. Available from: https://www.mdpi.com/2071-1050/13/8/4183.
60. Rozman U, Kalčíková G. Seeking for a perfect (non-spherical) microplastic particle – The most comprehensive review on microplastic laboratory research. J Hazard Mater. 2022;424:127529.
61. Hildebrandt L, Zimmermann T, Pröfrock D. Laser microdissection pressure catapulting (LMPC): a new technique to handle single microplastic particles for number-based validation strategies. Anal Bioanal Chem. 2023;415:3041–9.
62. Mitrano DM, Beltzung A, Frehland S, Schmiedgruber M, Cingolani A, Schmidt F. Synthesis of metal-doped nanoplastics and their utility to investigate fate and behaviour in complex environmental systems. Nat Nanotechnol. 2019;14:362–8.
63. Ruggero F, Gori R, Lubello C. Methodologies for Microplastics Recovery and Identification in Heterogeneous Solid Matrices: A Review. J Polym Environ. 2020;28:739–48.

Publisher's Note